ISSN 2176-5480

22nd International Congress of Mechanical Engineering (COBEM 2013)
November 3-7, 2013, Ribeirão Preto, SP, Brazil

COMPARATIVE ANALYSIS OF THE SLIDER CRANK MECHANISM WITH AND WITHOUT CONTACT/FRICTION AT REVOLUTE JOINT CLEARANCE

Vitor Luiz Reis
Katia Lucchesi Cavalca
University of Campinas – Campinas - Brazil
vreis88@gmail.com; katia@fem.unicamp.br

Abstract. *This work presents the development of a dynamic model for the slider-crank mechanism with clearance on the piston-pin revolute joint. The equations of motion for this system are obtained by Lagrange's method and the effects related to contact, friction and lubrication at the elements that operate in the clearance are also included. The dynamic behavior of a system in which the contact, friction and lubrication forces are modeled is compared to a previous simplified model with no contact force accounted on it. The contact force model used in this work is based on Hertz formulation, considering the dissipative effect associated with the pin impact against the piston. The frictional force model is based on the Coulomb friction but modeled by multibody dynamics approach. It was observed that when the contact force is accounted, the system response does not show discontinuities and the lubrication dynamic behavior is changed. By adding this contact force, it was concluded that its modeling plays an important role in the system response of mechanism in which the clearance is present at the revolute joint.*

Keywords: *slider-crank mechanism, revolute joint clearance, contact force, friction force, hydrodynamic lubrication*

1. INTRODUCTION

The slider-connecting rod joint is characterized as a revolute joint, highly applied in slider-crank mechanisms similar to the piston-pin joint in combustion engines, for example. However, as it involves an oscillatory motion, the lubrication model applied to this kind of joint must be carefully investigated when the clearance is considered in the joint. In this case, the clearance is filled with a lubricant that generates a pressure distribution and, consequently, hydrodynamic forces actuating in the components of the mechanical system. Some authors have been investigating the dynamic behaviour of mechanisms considering the lubrication at the clearance joints.

Schwab et al. (2002) compared different revolute joint clearance models in the dynamic analysis of rigid and elastic mechanical systems. The hydrodynamic lubrication model, in this case, considered the finite length of the bearing and the effect of cavitation in the fluid film.

Flores et al. (2004) accomplished a dynamic analysis of a mechanical system with lubricated joints, applying a hydrodynamic lubrication model to an infinitely long journal bearing, taking into account the hydrodynamic forces due to only squeeze effects. However, for high angular velocities, the simple squeeze approach is not valid and, consequently, the Reynolds equation should be applied. Flores et al. (2006) continued the study on dynamics of mechanical systems including joints with clearance with a hydrodynamic lubrication model based on the solution of the Reynolds equation, considering the infinitely long journal bearing condition, besides squeeze and wedge effects.

Flores et al. (2009) presented a general methodology for the lubricated revolute joints modelling in constrained rigid multibody systems.

Tian et al. (2010) simulated the behavior of planar flexible multibody systems with clearance and lubricated revolute joints. For lubricated revolute joints, the hydrodynamic forces were calculated as proposed by Flores et al. (2009). However, aiming to consider possible cavitation effects, some modifications were done in the lubrication model as proposed by Ravn et al. (2000).

Daniel and Cavalca (2011) analyzed the dynamic of a slider–crank mechanism with hydrodynamic lubrication in the connecting rod–slider joint clearance. The hydrodynamic lubrication model was previously developed by Bannwart et al. (2010) and it considered the infinitely long journal bearing condition. The hydrodynamic forces were obtained due to wedge effects.

Finally, Machado et al. (2012) studied the effect of the lubricated revolute joint parameters and hydrodynamic force models on the dynamic response of planar multibody systems. This way, three different hydrodynamic force models were considered, being the Pinkus and Sternlicht (Pinkus and Sternlicht, 1961) model for infinitely long journal-bearings and the Frêne et al. (1997) models for infinitely long and short journal-bearings. According the results obtained in the simulations, the hydrodynamic force models changed the dynamic characteristics of the multibody systems. Therefore, the lubrication model applied in the piston-pin system analysis should be carefully chosen.

ISSN 2176-5480

2. DYNAMICAL MODEL OF THE MECHANISM

A planar slider-crank mechanism is shown in Figure 1. This mechanism is widely used in machines like internal combustion engines and it is modelled to have a revolute joint clearance at the slider. This cylindrical joint attaches the connecting rod pin (in black) to the slider. The mechanism has three degrees of freedom (or independent co-ordinates): the crank angular displacement (q); the connecting rod angular displacement (A) and the slider horizontal position (X_{PT}).

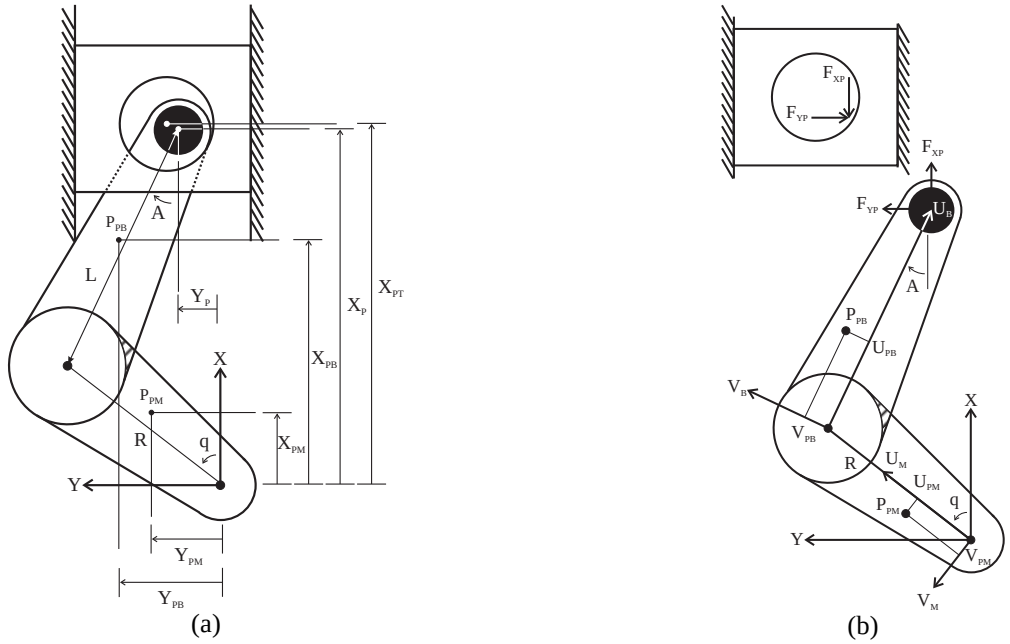

Figure 1. Slider-crank mechanism: (a) coordinate system; (b) centres of masses and coupling loads.

From Figure 1(a), the following geometric parameters are defined: the crank length (R); and the length of the connecting rod (L). The position of the center of the pin (X_P, Y_P) and its velocity at inertial frame ($\dot{X}_P, \dot{Y}_P$) are calculated from expressions Eq. (1) and (2), respectively (Doughty, 1988).

$$\begin{Bmatrix} X_p \\ Y_p \end{Bmatrix} = \begin{Bmatrix} Rcos(q) + Lcos(A) \\ Rsin(q) - Lsin(A) \end{Bmatrix} \tag{1}$$

$$\begin{Bmatrix} \dot{X}_p \\ \dot{Y}_p \end{Bmatrix} = \begin{bmatrix} -Rsin(q) & -Lsin(A) \\ Rcos(q) & -Lcos(A) \end{bmatrix} \begin{Bmatrix} \dot{q} \\ \dot{A} \end{Bmatrix} \tag{2}$$

In order to evaluate the equation of motion of the subsystem composed by the crank and the connecting rod, a kinematic analysis of the centre of mass of these bodies is required. Figure 1(b) shows the position of these points of interest on each component of the subsystem and the coupling loads that arise from the modelling of the clearance.

According to Figure 1(b), U_{PM} and V_{PM} are the mass centre coordinates of the crank (P_{PM}) in the referential system located in the crank (U_M, V_M), U_{PB} and V_{PB} are the centre of mass coordinates of the connecting rod (P_{PB}) in the reference frame located in the connecting rod (U_B, V_B), X_{PM} and Y_{PM} are the linear displacements of the centre of mass of the crank (P_{PM}) in the inertial referential system (X, Y) and X_{PB} and Y_{PB} are the linear displacements of the centre of mass of the connecting rod (P_{PB}) in the inertial referential system (X, Y), respectively (Doughty, 1988).

The position for the crank centre of mass is:

$$\begin{Bmatrix} X_{PM} \\ Y_{PM} \end{Bmatrix} = \begin{Bmatrix} U_{PM}cos(q) - V_{PM}sin(q) \\ U_{PM}sin(q) + V_{PM}cos(q) \end{Bmatrix} \tag{3}$$

ISSN 2176-5480

Similarly, the position of the connecting rod centre of mass is:

$$\begin{Bmatrix} X_{PB} \\ Y_{PB} \end{Bmatrix} = \begin{Bmatrix} Rcos(q) + U_{PB}cos(A) + V_{PB}sin(A) \\ Rsin(q) - U_{PB}sin(A) + V_{PB}cos(A) \end{Bmatrix} \tag{4}$$

Figure 1(b) also presents the coupling forces (F_{xp} and F_{yp}) applied to the mechanism. The generalized components of the force applied on the subsystem crank-connecting rod are:

$$\begin{Bmatrix} Q_q \\ Q_A \end{Bmatrix} = \begin{Bmatrix} F_{yp}Rcos(q) - F_{xp}Rsin(q) \\ -F_{yp}Lcos(A) - F_{xp}Lsin(A) \end{Bmatrix} \tag{5}$$

Considering M_M and M_B as the crank and the connecting rod masses, respectively; and g as gravity acceleration, the potential energy of this subsystem can be written as:

$$V = g\left(M_M X_{PM} + M_B X_{PB}\right) \tag{6}$$

The piston equation of motion is obtained by the force balance, resulting in:

$$M_{PT}\ddot{X}_{PT} = -\left(gM_{PT} + F_{xp}\right) \tag{7}$$

Defining I_{M0} e I_B as the crank rotational inertia in relation to inertial reference frame, and the connecting rod rotational inertia, the complete equation of motion (Eq. 8) for this mechanism with clearance is obtained applying the second form of Lagrange Method (Daniel and Cavalca, 2011; Doughty, 1988).

$$\begin{aligned} &\begin{bmatrix} M_B R^2 + I_{M0} & -M_B R\left(U_{PB}cos\left(A+q\right) + V_{PB}sin\left(A+q\right)\right) \\ sym & M_B\left(U_{PB}^2 + V_{PB}^2\right) + I_B \end{bmatrix}\begin{Bmatrix} \ddot{q} \\ \ddot{A} \end{Bmatrix} + \\ &+M_B R(V_{PB}cos(A+q) - U_{PB}sin(A+q))\begin{bmatrix} \dot{q}^2 & 0 \\ 0 & \dot{A}^2 \end{bmatrix} + \\ &+g\begin{Bmatrix} M_M\left(-U_{PM}sin(q) - V_{PM}cos(q)\right) - M_B Rsin(q) \\ M_B\left(-U_{PB}sin(A) + V_{PB}cos(A)\right) \end{Bmatrix} = \begin{Bmatrix} F_{yp}Rcos(q) - F_{xp}Rsin(q) \\ -F_{yp}Lcos(A) - F_{xp}Lsin(A) \end{Bmatrix} \\ &M_{PT}\ddot{X}_{PT} = -\left(gM_{PT} + F_{xp}\right) \end{aligned} \tag{8}$$

2.1 Relative motion between connecting rod and piston

The equation of motion obtained in the last section presents the typical case of coupling in multibody system with clearances. In such systems the kinematic constraints are replaced by force constraints (e.g. F_{xp} and F_{yp}). The evaluation of the magnitude of these forces and their directions are based on relative motion between the connecting rod and the piston (Flores et al. 2004).

Defining the radial clearance (c_r) as the difference between the journal radius (pin) and the bearing radius (hole on the slider), and the relative distance between their centers position as eccentricity vector (e), it's possible to determine if these bodies are in contact or not.

According to Figures 1 and 2(a) the components of the eccentricity vector are calculated as:

$$\mathrm{e} = \begin{Bmatrix} e_x \\ e_y \end{Bmatrix} = \begin{Bmatrix} X_p - X_{PT} \\ Y_p - Y_{PT} \end{Bmatrix} \tag{9}$$

When the impact occurs, the normal penetration depth δ is calculated as:

$$\delta = e - c_r \tag{10}$$

ISSN 2176-5480

Figure 2. Representation of contact (a) and Lubrication (b)

The eccentricity ratio (ε) is defined as the ratio of eccentricity by radial clearance:

$$\varepsilon = \frac{e}{c_r} \tag{11}$$

The time rate of eccentricity ratio variation, denoted by $\dot{\varepsilon}$, is obtained by differentiating the Eq. (11) with respect to time:

$$\dot{\varepsilon} = \frac{\dot{e}}{c_r} \tag{12}$$

The γ angle, shown in Figure 2(a), is calculated as:

$$\gamma = atan2\left(\frac{e_y}{e_x}\right) \tag{13}$$

And its derivate with respect to time is calculated as follows:

$$\dot{\gamma} = \frac{e_x\dot{e}_y - e_y\dot{e}_x}{e^2} \tag{14}$$

To calculate the relative velocities in which the bodies interact, it's necessary to find the point along the eccentricity line where the process of contact occurs. The position of this point is calculated as follows:

$$\begin{aligned} X_k^c &= X_k + R_k cos(\gamma) \\ Y_k^c &= Y_k + R_k sin(\gamma) \end{aligned} \quad k = i, j \tag{15}$$

Where R_i and R_j represents the journal and the bearing radius. The velocity of the point of contact is calculated as:

$$\begin{aligned} \dot{X}_k^c &= \dot{X}_k - \dot{\gamma}R_k sin(\gamma) \\ \dot{Y}_k^c &= \dot{Y}_k + \dot{\gamma}R_k cos(\gamma) \end{aligned} \quad k = i, j \tag{16}$$

And the relative scalar velocities of these bodies are:

$$\begin{aligned} \dot{X}_{rel}^c &= \dot{X}_j^c - \dot{X}_i^c \\ \dot{Y}_{rel}^c &= \dot{Y}_j^c - \dot{Y}_i^c \end{aligned} \tag{17}$$

Finally the relative normal and tangential velocities to the plane of collision are calculated:

ISSN 2176-5480

$$\begin{aligned} v_N &= \dot{X}^c_{rel}\cos(\gamma) + \dot{Y}^c_{rel}\sin(\gamma) \\ v_T &= -\dot{X}^c_{rel}\sin(\gamma) + \dot{Y}^c_{rel}\cos(\gamma) \end{aligned} \tag{18}$$

3. CONTACT AND FRICTION'S FORCE MODELS

The contact force model used in this application was proposed by Lankarani and Nikravesh (1994). This model is widely used in mechanical simulations of multibody mechanisms with clearances (Machado et al., 2012a). In this model the contact force includes a dissipative term, proportional to the impact velocity of the bodies, and although it has been developed for spheres collision, it is commonly used for cylindrical contact (Machado et al., 2012a). According to this formulation, the normal force acting on the bodies in contact is:

$$F_N = K\delta^n + D\dot{\delta} \tag{19}$$

where δ is the indentation, the exponent n depends on the of materials in contact, ($\dot{\delta}$) is the relative normal velocity of the bodies and K is the contact stiffness obtained by:

$$K = \frac{4}{3\left(\sigma_i + \sigma_j\right)}\left[\frac{R_i R_j}{R_i + R_j}\right]^{\frac{1}{2}} \tag{20}$$

The parameter σ_k is calculated as follows:

$$\sigma_k = \frac{1 - \nu^2}{E_k}\left[\frac{R_i R_j}{R_i + R_j}\right]^{\frac{1}{2}} \qquad k = i, j \tag{21}$$

with ν being the Poisson ratio and E the Young modulus of the materials in contact. The parameter D that controls the dissipation energy in the contact is obtained by:

$$D = \frac{3K\left(1 - c_e\right)^2}{4\dot{\delta}^{(-)}}\delta^n \tag{22}$$

where c_e is the restitution coefficient and $\dot{\delta}^{(-)}$ is the impact velocity. The final expression for normal contact force is:

$$F_N = K\delta^n\left[1 + \frac{3\left(1 - c_e\right)^2}{4}\frac{\dot{\delta}}{\dot{\delta}^{(-)}}\right] \tag{23}$$

The friction force model used in the simulations is based on Coulomb friction theory (Ambrosio, 2003). It can be expressed as follows:

$$F_T = -c_f c_d F_N \frac{v_T}{\mathrm{v}_T} \qquad c_d = \begin{cases} 0 & \text{if } \mathrm{v}_T < \mathrm{v}_0 \\ \dfrac{\mathrm{v}_T - \mathrm{v}_0}{\mathrm{v}_1 - \mathrm{v}_0} & \text{if } \mathrm{v}_0 < \mathrm{v}_T < \mathrm{v}_1 \\ 1 & \text{if } \mathrm{v}_T > \mathrm{v}_1 \end{cases} \tag{24}$$

In which c_f is a friction coefficient, c_d is a dynamic coefficient dependent on the relative velocity of sliding between two bodies, v_T is a tangential velocity and v_T is its modulus, v_0 and v_1 are the given tolerances for sliding velocity.

4. LUBRICATION MODEL

The adopted lubrication model considers the alternating rotational motion in the journal bearing of the connecting rod-slider joint and the motion of the bearing fixed in the slider (Bannwart et al., 2010). In this case, the tangential (angular) and radial velocities in the oil film have an imaginary part due to the oscillating motion of the connecting rod pin in both

ISSN 2176-5480

directions (Daniel and Cavalca, 2011). This lubrication model assumes that the fluid velocity in the axial coordinate is practically nil, as an infinitely long bearing. Moreover, the fluid is considered incompressible and Gümbel's cavitation condition is considered. Therefore, the velocity field presented in this model is obtained from Eq. (25).

$$V_\theta(y,\theta) = \frac{U_0 \sinh\left(h(\theta) - y\sqrt{\frac{i\dot{q}}{\upsilon}}\right)}{\sinh\left(h(\theta)\sqrt{\frac{i\dot{q}}{\upsilon}}\right)} + \frac{\upsilon}{i\dot{q}\mu R_i}\frac{dP_t}{d\theta}\left\{\frac{\sinh\left(h(\theta) - y\sqrt{\frac{i\dot{q}}{\upsilon}}\right) + \sinh\left(y\sqrt{\frac{i\dot{q}}{\upsilon}}\right)}{\sinh\left(h(\theta)\sqrt{\frac{i\dot{q}}{\upsilon}}\right)} - 1\right\} \tag{25}$$

The variables U_0, $\dot{q}$, R_i, h, υ and μ are the linear velocity in the shaft surface, the rotational speed of the crank, the bearing radius, the fluid film thickness, the kinematic viscosity, and the absolute viscosity, respectively. Considering the condition $P(0) = P(2\pi) = 0$, the pressure distribution is presented as:

$$P(\theta) = P_0 + \rho\dot{q}R_iU_0\left\{\frac{L}{R_i}\left[1 - \cos(\theta)\right] - \theta i\right\} + \mu R_iU_0\frac{i\dot{q}}{\upsilon}\int_0^\theta \frac{\tanh\left[\frac{h(\theta)}{2}\sqrt{\frac{i\dot{q}}{\upsilon}}\right] - K_1\frac{c_r}{2}\sqrt{\frac{i\dot{q}}{\upsilon}}}{h(\theta)\sqrt{\frac{i\dot{q}}{\upsilon}} - 2\tanh\left[\frac{h(\theta)}{2}\sqrt{\frac{i\dot{q}}{\upsilon}}\right]}d\theta \tag{26}$$

where ρ is the oil density and K_1 is defined as:

$$K_1 = \int_0^{2\pi}\left\{\frac{\tanh\left[\frac{h(\theta)}{2}\sqrt{\frac{i\dot{q}}{\upsilon}}\right]}{h(\theta)\sqrt{\frac{i\dot{q}}{\upsilon}} - 2\tanh\left[\frac{h(\theta)}{2}\sqrt{\frac{i\dot{q}}{\upsilon}}\right]} - 1\right\}d\theta \Big/ \frac{c_r}{2}\sqrt{\frac{i\dot{q}}{\upsilon}}\int_0^{2\pi}\frac{d\theta}{h(\theta)\sqrt{\frac{i\dot{q}}{\upsilon}} - 2\tanh\left[\frac{h(\theta)}{2}\sqrt{\frac{i\dot{q}}{\upsilon}}\right]} \tag{27}$$

Finally, the hydrodynamic forces of the fluid film acting on the journal ($y = h$) are:

$$F_x = wR_j\int_0^{2\pi}\left(-P\sin(\theta) + \mu\frac{\partial V_\theta}{\partial y}\cos(\theta)\right)_{y=h}d\theta \tag{28}$$

$$F_y = wR_j\int_0^{2\pi}\left(-P\cos(\theta) + \mu\frac{\partial V_\theta}{\partial y}\sin(\theta)\right)_{y=h}d\theta \tag{29}$$

The resultant forces are written in the inertial frame (X,Y) applying the following coordinate transformation:

$$\begin{Bmatrix} F_Y \\ F_X \end{Bmatrix} = \begin{Bmatrix} F_y\sin(\gamma) - F_x\cos(\gamma) \\ F_y\cos(\gamma) + F_x\sin(\gamma) \end{Bmatrix} \tag{30}$$

This model covers the hydrodynamic lubrication condition. When a transition from lubrication to contact occurs, the pressure developed in a fluid film approaches to a Hertzian contact pressure distribution. In order to minimize effects of a rough transition between lubrication and contact, a scheme presented in Eq. (31) is used (Flores et al., 2004).

$$F = \begin{cases} F_{lubricated} & if\ e \le c_r \\ \frac{(c_r + e_0) - e}{e_0}F_{lubricated} + \frac{e - c_r}{e_0}F_{dry} & if\ c_r \le e \le c_r + e_0 \\ F_{dry} & if\ e \ge c_r + e_0 \end{cases} \tag{31}$$

According to Eq. (31), the system is in hydrodynamic lubrication up to the radial clearance c_r, and the mixed lubrication condition (hydrodynamic + dry) is calculated considering the radial clearance boundary as $c_r + e_0$, which is the starting point to the dry contact transition. However, to guarantee the continuity in the force evaluation (avoiding

ISSN 2176-5480

jumps to infinite values) the radial clearance used in the forces evaluation is $c_r + e_0 + e_1$, where e_0 and e_1 are given tolerances to eccentricity, carefully chosen as function of radial clearance.

The dynamic equations developed in the last sections were integrated in time, using a Predictor-Corrector integrator, developed by Shampine and Gordon (1975), largely applied in dynamic simulations of nonlinear systems.

5. RESULTS

The dynamic response of the mechanism with clearance and lubrication are investigated and two modelling strategies are compared. The first one, denoted as hybrid model, was employed in a previous work (Daniel and Cavalca, 2011). It assumes that when the pin approaches to the contact and the eccentricity ratio (ε) becomes higher than 0.9, the system's dynamic behavior is governed by the conventional 1 degree of freedom (d.o.f.) slider-crank mechanism, with no clearance in the connecting rod-slider joint. Therefore, the conventional model of the slider-crank mechanism is used until a reverse motion occurs in the slider, when the slider pin leaves the bearing surface, shifting the lubrication condition to hydrodynamic.

The second approach developed in later sections, includes the effects contact/friction and ensures the continuity of the transition between lubrication and contact/friction models. These approaches are compared in numerical simulations. The physical and geometric properties of each component of the mechanism are listed in Table 1.

Table 1. Parameters of the Slider-Crank Mechanism.

Parameter	Unit	Symbol	Value
Crank Length	[m]	R	0.0508
Connecting Rod Length	[m]	L	0.2032
Crank Inertia	[kg.m]	I_M	0.006
Connecting Rod Inertia	[kg.m]	I_B	0.010
Crank Mass	[kg]	M_M	0.8
Connecting Rod Mass	[kg]	M_B	1.36
Slider Mass	[kg]	M_{pt}	0.910
Position of the Crank Center of Mass in the axis U_M	[m]	U_{PM}	0
Position of the Crank Center of Mass in the axis V_M	[m]	V_{PM}	0
Position of the Connecting Rod Center of Mass in the axis U_B	[m]	U_{PB}	0.0508
Position of the Connecting Rod Center of Mass in the axis V_B	[m]	V_{PB}	0

The parameters used to characterize the effect of contact/friction forces and the lubrication models are listed in Table 2. The global results reported correspond to two full crank cycles. The initial conditions for all simulations were obtained from ideal mechanism in steady-state regime and the initial eccentricity was set at zero.

Table 2. Parameters used in contact/friction and lubrication models of a piston-pin system.

Parameter	Unit	Symbol	Value
Piston-pin Radius	[mm]	R_i	10.00
Restitution Coefficient		c_e	0.90
Friction Coefficient		c_f	0.03
Contact Exponent		n	1.50
Young Modulus	[GPa]	E	207
Poisson Ratio		ν	0.30
Absolute Viscosity	[Pa.s]	μ	0.0117
Oil Density	[kg/m^3]	ρ	887.8
Hydrodynamic Bearing Width	[m]	w	0.015
Error Tolerance (Integration)			$1.00\ 10^{-6}$
Maximum Step-size (Integration)	[s]		$1.00\ 10^{-7}$

5.1 Simulation I

The first simulation analyzes the dynamic behavior of the mechanism with clearance in comparison to the ideal joint (1 DOF). For this purpose, the maximum velocity of the crank is 250rad/s and the piston-pin clearance is 20μm.

In Fig. 3 the angular velocity of the crank for both models are compared. The hybrid model (Fig. 3a) approaches to the behavior of ideal joint while the lubrication + contact/friction model (Fig. 3b) presents a small offset in comparison to ideal mechanism. This occurs because the lubrication and the contact models dissipate energy in the system.

ISSN 2176-5480

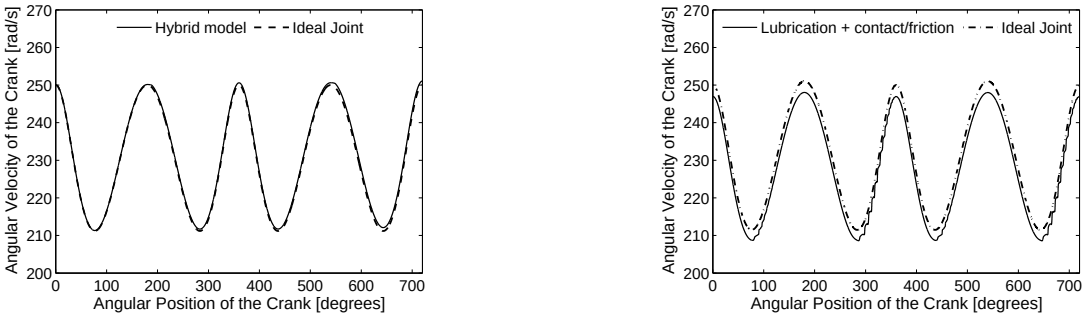

Figure 3. Angular Velocity of the Crank: (a) Hybrid model; (b) Lubrication + contact/friction

The acceleration of the slider was also investigated. It was observed that hybrid model in Fig. 4(a) shows small oscillations around the ideal mechanism response. This occurs because in the most part of the time the piston-pin is in contact with the slider. For the proposed model, the slider acceleration presents more significative disturbances (Fig. 4(b)) as a consequence of the transition of the lubrication to the contact/friction models.

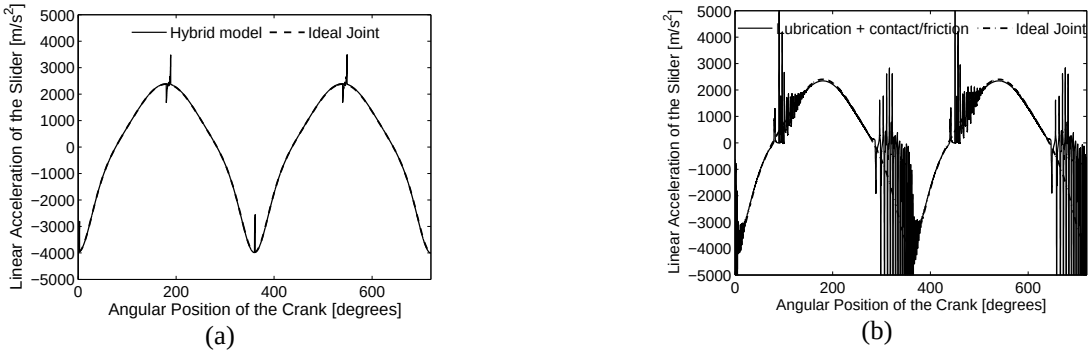

Figure 4. Linear Acceleration of the Slider: (a) Hybrid model; (b) Lubrication + contact/friction

Figure 5(a) shows the piston pin trajectory normalized by radial clearance for the hybrid model. Again it can be observed that the pin was in contact most part of the cycle and for the lubrication + contact/friction model the transition between these force models occurs many times during the simulation.

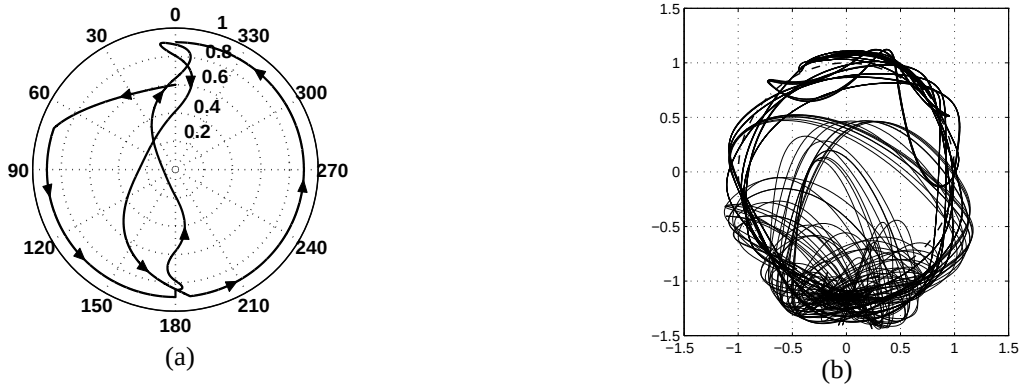

Figure 5. Journal center trajectory: (a) Hybrid model; (b) Lubrication + contact/friction

5.2 Simulation II

In the second simulation the radial clearance is set to 40μm and the other parameters are maintained unchanged. In Fig. 6(a) the angular velocity of the crank shows that the response of the hybrid model moves away from the ideal behavior. The model with contact/friction shows the increase of the offset (Fig. 6(b)) previously observed in the last simulation.

ISSN 2176-5480

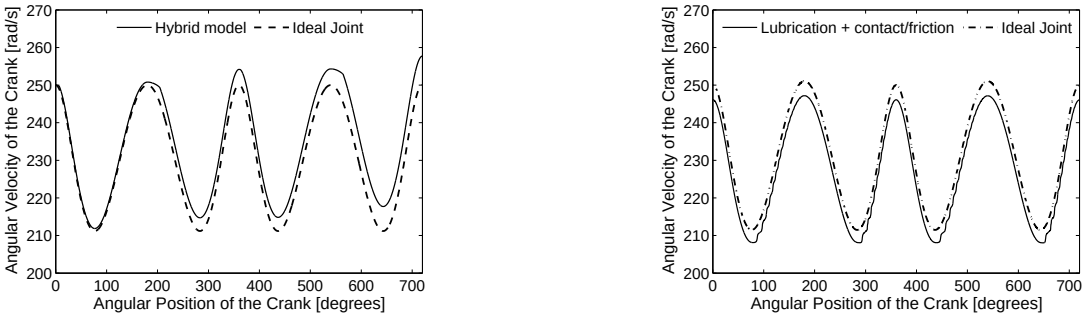

Figure 6. Angular Velocity of the Crank: (a) Hybrid model; (b) Lubrication + contact/friction

The slider acceleration for the hybrid model showed in Fig. 7(a) reveals even small oscillations around the ideal mechanism response in comparison to the smaller clearance. However, the proposed model in Fig. 7(b) shows that the increase of the clearance implies in major losses in the mechanism performance.

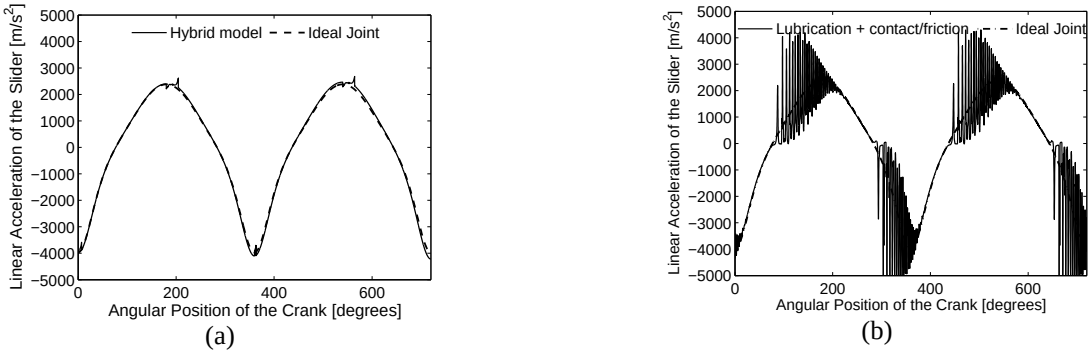

Figure 7. Linear Acceleration of the Slider: (a) Hybrid model; (b) Lubrication + contact/friction

In Figure 8(a) it can be observed that the trajectory of the pin was not significantly affected by the increase of the clearance. However, in Fig. 8(b) the trajectory of the pin has changed and it stayed in contact for the most part of the time during the simulation.

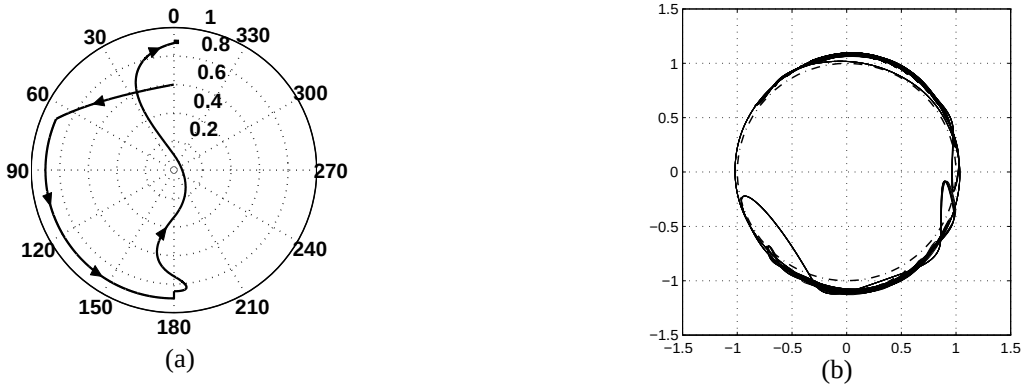

Figure 8. Journal center trajectory: (a) Hybrid model; (b) Lubrication + contact/friction

5.3 Simulation III

The simulation investigates the mechanism response when the maximum velocity of the crank is increased to 1,000rad/s, while the others parameters are maintained constant. In this condition the hybrid model shows the same trend observed when the clearance size increased, Fig. 9(a). A similar behavior also occurs in the model that takes in account the friction and contact forces, Fig. 9(b).

ISSN 2176-5480

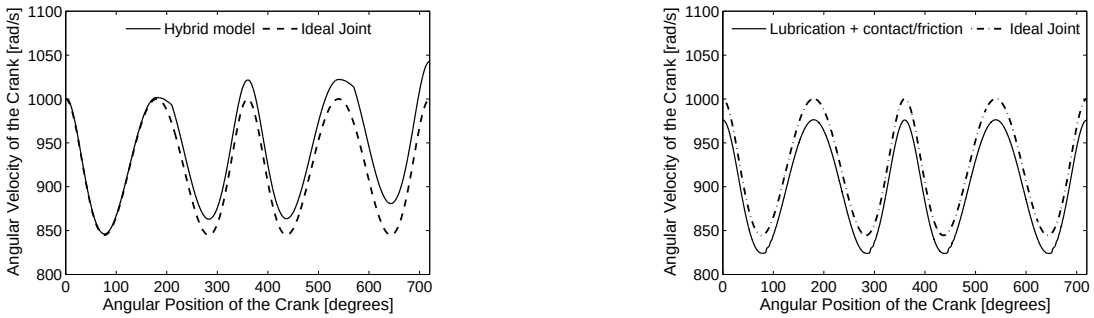

Figure 9. Angular Velocity of the Crank: (a) Hybrid model; (b) Lubrication + contact/friction

The analysis of the slider acceleration in Figs. 10(a-b) for both models shows that the hybrid one has a response that approaches to ideal mechanism. The model considering lubrication and contact/friction forces has a similar behavior to ideal mechanism too. This occurs because the piston-pin is in contact with the bearing practically the whole time in the simulation.

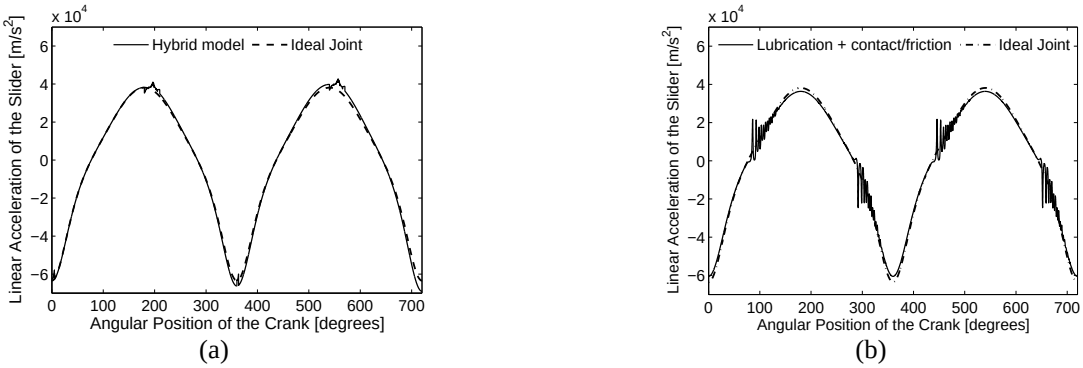

Figure 10. Linear Acceleration of the Slider: (a) Hybrid model; (b) Lubrication + contact/friction

Figs. 11(a-b) present the journal center trajectory predicted for the piston pin. In the hybrid model it was observed the alternate between contact and lubrication regime, which indicates that the hydrodynamic lubrication was not capable of sustaining the pin in this regime during the simulations. Following the same trend, the proposed model in Fig. 11(b) shows that the pin remains in contact with high indentation deep as a consequence of the high velocities developed in the mechanism.

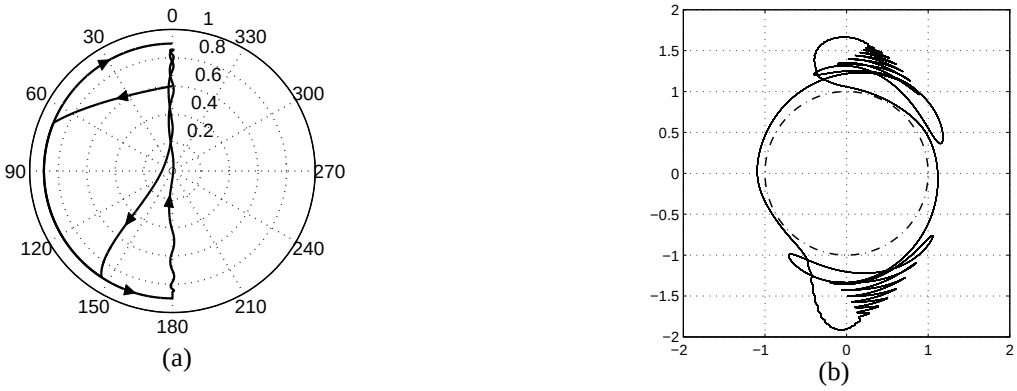

Figure 11. Journal center trajectory: (a) Hybrid model; (b) Lubrication + contact/friction

ISSN 2176-5480

6. CONCLUDING REMARKS

The present paper discussed the impact of the inclusion of the contact and friction forces in the dynamic model developed to analyze the response of the slider-crank with revolute joint clearance. The comparison between the previous hybrid model and the model proposed here shows the influence and the significance of taking into account the contact/friction forces in the dynamic response of this mechanism.

In order to improve the modeling of the system, the results also point out the importance of the development of an elastohydrodynamic lubrication scheme to predict more accurately the complex lubrication regime present in these machines.

7. ACKNOWLEDGEMENTS

The authors would like to thank CNPq and CAPES for the financial support of this work.

8. REFERENCES

Ambrósio, J., 2003. “Impact of Rigid and Flexible Multibody Systems: Deformation Description and Contact Models”. *Virtual Nonlinear Multibody Systems*, (Michael Valasek, Werner Schiehlen, eds.), Kluwer Academic Publishers, Dordrecht, Netherlands, p. 57–81.

Bannwart, A. C., Cavalca, K. L. and Daniel, G. B., 2010. “Hydrodynamic bearings modeling with alternate motion”. *Mechanics Research Communications*, Vol. 37, p. 590-597.

Daniel, G. B. and Cavalca, K. L., 2011. “Analysis of the dynamics of a slider-crank mechanism with hydrodynamic lubrication in the connecting rod-slider joint clearance”. *Mechanism and Machine Theory*, Vol. 46, p. 1434-1452.

Doughty, S., 1988. *Mechanics of Machines*. John Wiley & Sons.

Flores, P., Ambrósio, J. and Claro, J.P., 2004. “Dynamic analysis for planar multibody mechanical systems with lubricated joints”. *Multibody Syst. Dyn.*, Vol. 12, p. 47–74.

Flores, P., Ambrósio, J., Claro, J., Lankarani, H. and Koshy, C., 2006. “A study on dynamics of mechanical systems including joints with clearance and lubrication”. *Mechanism and Machine Theory*, Vol. 41, p. 247-261.

Flores, P., Ambrósio, J., Claro, J., Lankarani, H. and Koshy, C., 2009. “Lubricated revolute joints in rigid multibody systems”. *Nonlinear Dynamics*, Vol. 56, p. 277-295.

Frêne, J., Nicolas, D., Degneurce, B., Berthe, D. and Godet, M., 1997. *Hydrodynamic Lubrication-Bearings and Thrust Bearings*. Elsevier, Amsterdam.

Lankarani, H.M., and Nikravesh, P.E., 1994. “Continuous Contact Force Models for Impact Analysis in Multibody Systems”. *Nonlinear Dynamics*, Vol. 5, p. 193-207.

Machado, M., Moreira, P., Flores, P. and Lankarani, H.M., 2012a. “Compliant contact force models in multibody dynamics: Evolution of the Hertz contact theory”. *Mechanism and Machine Theory*, Vol. 53, p. 99–121.

Machado, M., Costa, J., Seabra, E. and Flores, P., 2012b. “The effect of the lubricated revolute joint parameters and hydrodynamic force models on the dynamic response of planar multibody systems”. *Nonlinear Dynamics*, Vol. 69, p. 635–654.

Pinkus, O. and Sternlicht, S.A., 1961. *Theory of Hydrodynamic Lubrication*. McGraw-Hill, New York.

Ravn, P., Shivaswamy, S., Alshaer, B.J. and Lankarani, H.M., 2000. “Joint clearances with lubri-cated long bearings in multibody mechanical systems”. *J. Mech. Des*. Vol. 122, p. 484–488.

Schwab, A.L. Meijaard, J.P. and Meijers, P., 2002. “A comparison of revolute joint clearance model in the dynamic analysis of rigid and elastic mechanical systems”. *Mechanism and Machine Theory*, Vol. 37(9), p. 895–913.

Shampine, L. F. and Gordon, M. K., 1975. *Computer Solution of Ordinary Differential Equations: The Initial Value Problem*. W.H.Freeman & Co Ltd.

Tian, Q., Zhang, Y., Chen, L. and Yang, J., 2010. “Simulation of planar flexible multibody systems with clearance and lubricated revolute joints”. *Nonlinear Dynamics*, Vol. 60, p. 489–511.

9. RESPONSIBILITY NOTICE

The authors are the only responsible for the printed material included in this paper.